J. Geotech. Eng., JSCE, No. 624/III-47, 21-30, 1999 June

NUMERICAL SIMULATION OF GROUTING BY TWO GROUT ANALYSIS METHODS

Muneo HORI[1]and Takanobu KOYAMA[2]

[1]Earthquake Research Institute, University of Tokyo (Yayoi, Bunkyo, Tokyo 113-0032, Japan)
[2]Tokyo Gas Co., Ltd. (Kaigan, Minato, Tokyo 105-0022, Japan)

This paper examines the validity of the Monte-Carlo simulation of fracture networks (MSFN) and the real-time inversion analysis (RTIA). The MSFN is applied to simulate the consolidation grouting and curtain grouting. Fairly good agreement with observed data is obtained for the relation between the pressure and amount of grout agents, 2) the spacial variation of Legion values, and 3) the appearance of grout agents in adjacent holes. The basic validity of the RTIA is verified through simple examples. Then, it is shown that the RTIA can predict the water channel conditions and the grouting distance for the consolidation grouting.

Key Words *: grout analysis, permeable flow, fracture network, inversion*

1. INTRODUCTION

We presented the two analysis methods for grouting in the accompanying paper[4]. The first is a Monte-Carlo simulation of fracture network[1] (MSFN) which predicts the grouting effects for a presumed grouting specification from the permeable flow analysis of fracture networks generated according to the observed data, and the second is a real-time inversion analysis (RTIA) which evaluates the range and degree of the grout agent intrusion making best use of continuously measured the grouting pressure and the amount of flow. It should be emphasized here that these two analysis methods use data which are ordinarily measured as input parameters. Appendix summarizes the model and formulation of these methods briefly.

In this paper, we simulate consolidation grouting and curtain grouting using these analysis methods. The basic properties of the target cites are summarized in **Table 1**. The rock mass for the consolidation grouting has relatively dense distribution of cracks, and the permeability is high. The rock mass for the curtain grouting is less permeable, though there exist well-developed cracks and some regions with highest permeability. The detailed geological and hydrological data are shown when the simulation is made.

The main objective of the present paper is to examine the validity of the MSFN and the RTIA, comparing results of numerical simulation with actually measured data. For the MSFN, the t-P-Q relations, the spacial variation of Legion values and the locations of grout agent appearance are used. For the RTIA, the results compared with those of the MSFN, as data which can be used directly for the comparison are not available. The usefulness of these grout analysis methods is discussed. As one example of the application, the MSFN is used to the grout effects for different specifications in order to investigate most suitable specification.

The content of this paper is as follows: Sections 2 and 3 are for the MSFN applied to the consolidation and curtain grouting, respectively. Section 4 is for the RTIA applied to the curtain grouting of the same site as studied in Section 3. As mentioned, the MSFN and the RTIA are presented in Appendix; see also the original paper[4].

2. CONSOLIDATION GROUTING OF MSFN

We carry out the MSFN to simulate consolidation grouting; the geological data of major cracks observed in a target site are summarized in **Table 2**; ϕ and θ are the dip angle (measured as the N-direction being 0) and the strike angel, and d and h are the average spacing and crack-opening-displacement. Young's modulus and Poisson's ratio used in the MSFN are also cited. **Figure 1** shows the location of the pilot (P) and the first to the sixth grouting holes. Each grouting hole has six stages, denoted by Stage 1 to Stage 6; a grout hole is divided into several parts,

[1] See, for instacen, [5),1),2),8)]; see recent works of [6),9)] and [3)].

Table 1 Properties of Cite

	consoli.	curtain
depth [m]	0∼-30	0∼100
rock	granite	granite
permeability	relatively high	low except some regions

Table 2 Geological Data: Consolidation Grouting

ϕ[deg]	11∼26
θ[deg]	11∼29
d[/cm]	0.01
h[cm]	0.1
E[MPa]	1000
ν	0.3

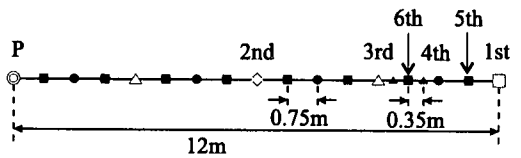

Fig. 1 Location of Grouting Holes

called stages, and each stage is sealed with packers at the top and bottom such that the pressure in the part becomes constant when grouting is applied.

As the stage length is 5[m], a circular cylindrical domain of radius 5[m] is used as a model of a target rock mass. Centers of fractures are randomly distributed in this region, and its strike and dip angles are randomly chosen from the ranges shown in **Table 2**.

(1) P-Q Relation for Legion Test

The MSFN needs to specify the joint radius, a, although other input parameters are determined from the geological data. The joint radius is determined by carrying out a parametric study to reproduce a Legion test of one stage. Stage 4 of the pilot hole is used in the parametric study. Four values of a shown in Table 3 are examined, and the average of P-Q relations of 100 simulations is plotted in **Fig. 2**; Q is set as the amount of flow per 1 minute and 1 meter of the stage length. As is seen, the P-Q relation changes depending on a, and $a = 150$[m] gives the closest relation to the measured one. This value is used in the following simulation.

The MSFN introduces three parameters, α, β and γ, which respectively account for the reduction of the elasticity due to grouting damage, the viscosity change due to stacking of grout agents, and the joint closing

Table 3 Parametric Study of a

case	1-1	1-2	1-3	1-4
a[cm]	75	100	150	200

Table 4 Parametric Study of α

case	2-1	2-2	2-3
α	0.25	0.5	0.75

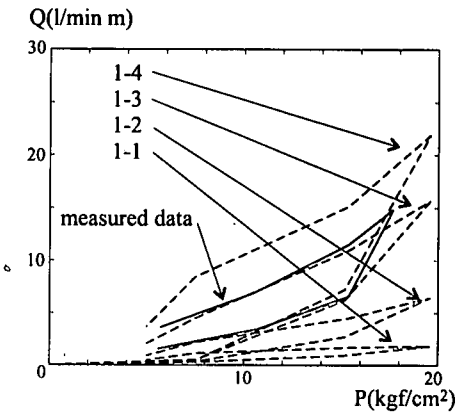

Fig. 2 Results of Parametric Study of a

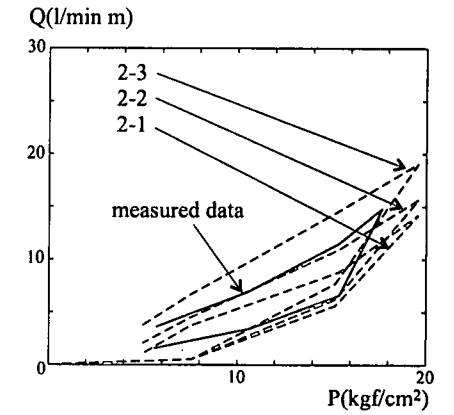

Fig. 3 Results of Parametric Study of α

due to the fulfillment of grout agents; see Appendix.

These parameters can be determined from a parametric study similar to the one for a. As an example, we present the parametric study for α. Three values of α shown in **Table 4** are examined, and the average P-Q relations are plotted in **Fig. 3**. The most suitable value among theses three is $\alpha = 0.5$; this means that the half of joint openings due to excessive pressure cannot be recovered when joints are damaged.

(2) t-Q Relation for Grouting

Two parameters, β and γ, are determined by using measured data of Stage 4 of the pilot and first grouting holes. Since β accounts for the effects of the intrusion time and the joint thickness on the hardening process, it can be determined by using one t-P-Q relation. However, γ requires at least two t-P-Q relations as it gives the decrease of the joint thickness for the amount of grout agents which was previously intruded. We use $\beta = 1$[cm/hour] and $\gamma = 0.05$[cm] in the present study. It should be emphasized that these parameters are determined from the measured t-P-Q relation of one stage of one grouting hole, and are used to reproduce data of other stages and other grouting holes. **Figure 4** compares the average t-Q relation of 100 simulations with the measured t-Q relation; a) is for Stage 4 of the pilot hole, from which β is determined, and b) is for Stage 4 of the first grouting hole, from which γ is determined. The measured t-P relation is used as input data. While detailed profiles are different, the average t-Q relation is fairly similar to the measured one even for the first grouting hole; in particular, the simulated total amount of the intruded grout differs less than 40% from the measured one for the first grouting hole. Such difference between the simulation and the observation may be negligible compared with the large variances in t-P-Q relations at different stages of the same grouting holes. Similar agreement is obtained for other stages and grouting holes.

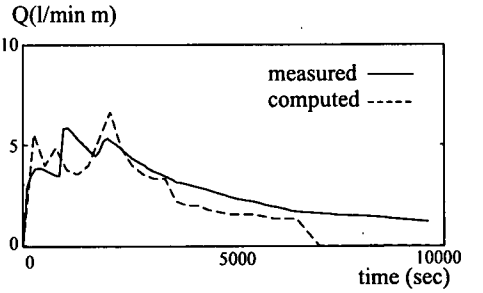

a) pilot hole

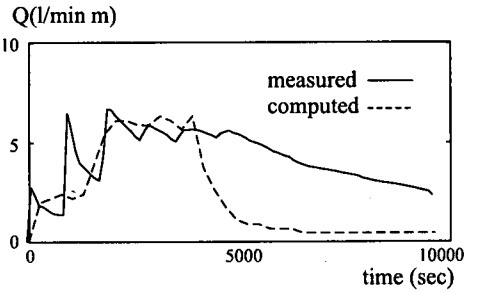

b) first grouting hole

Fig. 4 Computed t-Q Relation

(3) Grouting Effects

Since stages closer to the ground surface are damaged during the excavation, the crack-opening (h) and the Young moduli (E) are slightly changed from those used for deeper stages. **Table 5** shows the profile of stage 1 to 6 and the values[2] of h and E. The spatial variation of Legion values are obtained by carrying out fictitious Legion tests which use the same network with joint thickness reduced by the previous grouting. To this end, we first compute S, the saturation ratio of joints which is defined as the ratio of the intruded grout agent volume to the joint volume. This S determines the reduction of the joint thickness. The spacial variations of S for Stage 4 are shown in **Fig. 5**; since joints are randomly distributed, the isotropic distribution of S is assumed and S is plotted as a function of the distance. As the joint thickness is decreased, S tends to increase for later grouting holes.

Table 5 Parameters of Stage

stage	depth[cm]	h[cm]	E[kgf/cm^2]
1	30~530	0.3	3000
2	530~1030	0.2	3000
3	1030~1530	0.1	10000
4	1530~2030	0.1	10000
5	2030~2530	0.1	10000
6	2530~3030	0.1	10000

Average Legion values are computed for all stages in all grouting holes; see **Fig. 6**a) for shallower stages and **Fig. 6**b) for deeper stages. The measured Legion values are plotted for the comparison. While the values are different, the simulation yields similar tendency in decreasing Legion values with respect to the grouting hole. Indeed, the arrows indicate the grouting hole at which the measured Legion value becomes sufficiently small (less than 2). The simulation tells these grouting holes within the error of one grout hole; for Stage 1, for instance, the simulation shows that the fourth hole is the one at which the Legion value is small, and this coincides with the observation.

3. CURTAIN GROUTING OF MSFN

We carry out the MSFN to simulate curtain grouting which used one test hole divided into 20 stages. While most of stages had small Legion values, a Legion value of Stage 8, 11 or 16 was greater than 1000.

[2] These values are determined to reproduce Legion tests for each stage of the pilot hole.

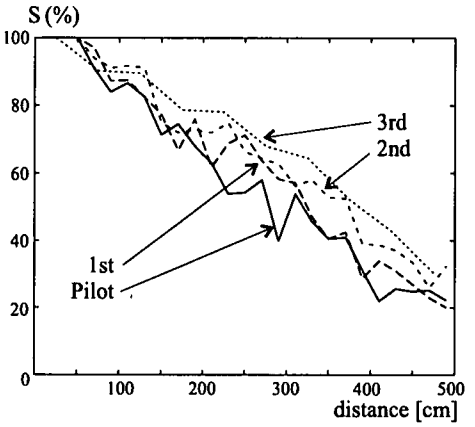

Fig. 5 Spacial Distribution of R

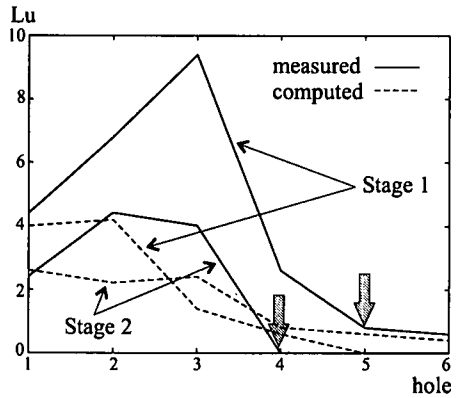

a) shallower stages

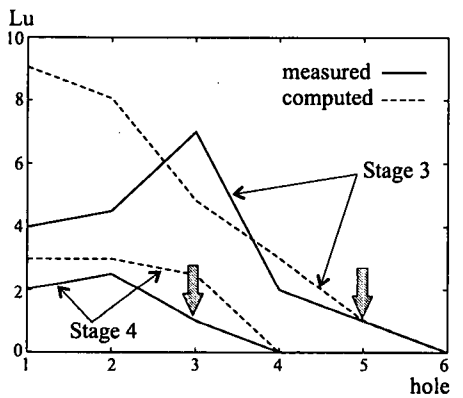

b) deeper stages

Fig. 6 Reduction of Lu

Well-developed cracks were observed in these stages. As a typical example, **Table 6** shows geological data of cracks observed in Stage 16; (ϕ, θ) are the strike and dip angles, z is the elevation and h is the mean crack-opening width. These stages are the target of the present analysis.

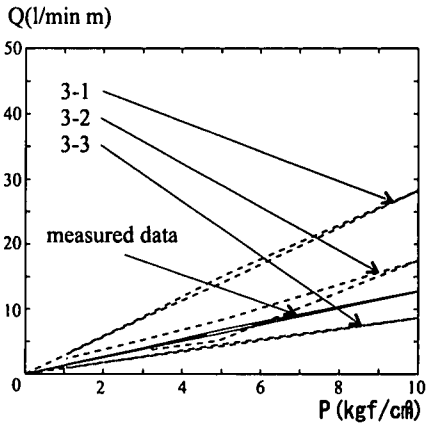

Fig. 7 Results of Parametric Study of a

Table 6 Geological Data: Curtain Grouting

	No. 1	No. 2	No.3	No. 4	No. 5
ϕ[deg]	67	63	45	40	70
θ[deg]	28	135	348	335	323
z[cm]	7625	7701	7763	8145	8160
h[cm]	0.16	0.08	0.09	0.09	0.09

Table 7 Parametric Study of a

case	3-1	3-2	3-3
a[cm]	80	100	120

A cylindrical domain of radius 5[m] is used as a model of one stage. Fractures are generated randomly on planes which correspond to the observed well-developed cracks; for instance, there are five planes for Stage 16.

(1) P-Q Relation for Legion Test

We first determine the joint radius, a, for this site using data of a Legion test. Three values of a shown in **Table 7** are examined, and the average P-Q relations are plotted in **Fig 7**. As is seen, $a = 100$[cm] is most suitable and used in the following analysis.

Since the grouting sites were located relatively deep, the deformation due to water pressure does not happen in the MSFN. Hence, the parameter α for this site cannot be determined.

(2) t-Q Relation for Grouting

We next determine the parameter β to reproduce data of grouting at Stage 16. Three values of β shown in **Table 8** are examined, and the average t-Q relations are ploted in **Fig. 8**. The sensitivity of the t-Q

Table 8 Parametric Study of β

case	4-1	4-2	4-3
β[cm/hour]	1.0	5.0	10.0

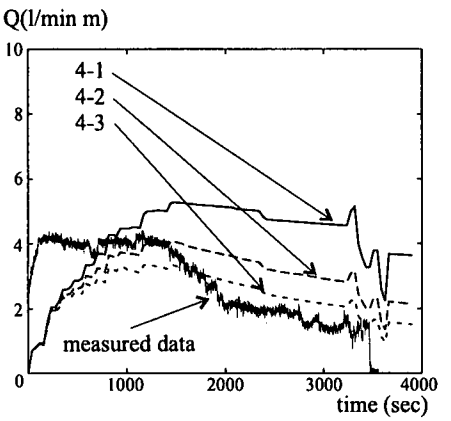

Fig. 8 Results of Parametric Study of β

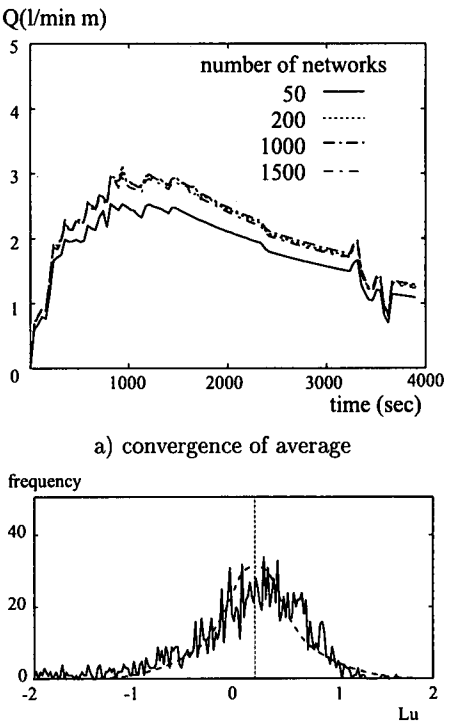

Fig. 9 Statistical Properties of Simulation Results

relation to β is clearly shown. While the decrease of Q (under a constant grout pressure) is reproduced, the simulated t-Q relation is fairly close to the observed one. As $\beta = 5$ predicts the total amount of the intruded grout best, this value is used in the following simulation.

Statistical information of permeable flows can be extracted from the MSFN; for instance, we can compute the standard deviation. As the comparison of the observation with the average is not quite satisfactory, we consider another comparison using the standard deviation. To this end, we first examine the convergence of the average relations, and show a typical example in **Fig. 9**a) which plots the average t-Q relations of 50 to 1500 simulations for Stage 16. It is seen that the average becomes more or less the same for more than 200 simulations. This relatively fast convergence is due to a log-normal distribution of Q at each time. The distribution of Q at 1000[sec] of 1500 simulations is plotted in **Fig. 9**b); a dashed curve is a log-normal distribution that is the closest to the distribution. Note that the log-normal distribution of Legion values are often reported; see, for instance, [7),10)]. This distribution of computed Q's may be another support of the validity of the MSFN.

Now, we compute the average and standard deviation of Q for Stages 16 and 11, in order to estimate the difference of the simulation from the observation based on the standard deviation. **Figure 10** plots the average and the standard deviation of the distribution of the t-Q relation which is assumed to be log-normal; (A) is the average, and (B) and (C) are the average plus and minus one standard deviation, respectively. The standard deviation is of the same order as the average, which may reflect the large variation in actual grouting. While the profile is different, the measured t-Q relations are bounded by (B) and (C), i.e., the average plus and minus one standard deviation, except for early periods. Assuming that Q obeys a log-normal distribution, we can expect that the MSFN reproduces actual data within the variation of one standard deviation.

(3) Appearance of Grout Agents

Next, we examine the validity of MSFN comparing the appearance of grout agents with the observed appearance. It should be noted that the appearance of grout agents changes depending on the direction since cracks are developed only in particular planes. Indeed, the saturation ratio, S, becomes anisotropic as shown in **Fig. 11** which plots S in eight directions from the grouting hole; 0 and 180[deg] correspond to the direction of curtain grout extension (0 to the left and 180 to the right).

There are two check holes in the 0 and 180 directions with distance 4.5[m] from the test hole. The MSFN can predict whether grout agents appear in these check

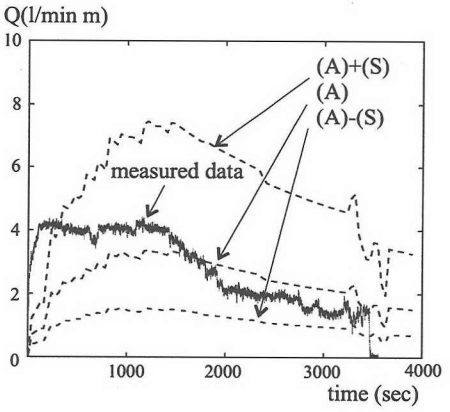

a) stage 16

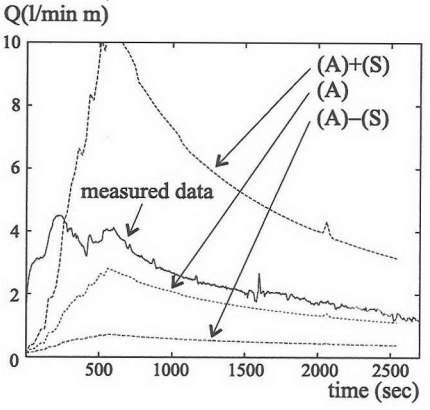

b) stage 11

Fig. 10 Example of Variation in Flow

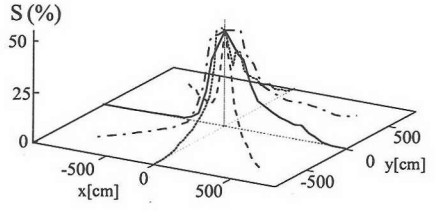

Fig. 11 Anisotropic Distribution of S

holes. **Figure 12** shows the probabilistic distribution of S at various elevations; S is classified into the four categories, $0 = S$, $0 < S < \frac{1}{3}$, $\frac{1}{3} < S < \frac{2}{3}$, $\frac{2}{3} < S < 1$, for simplicity. Assuming that the grout agents appears if the probability of $\frac{2}{3}$S1 is non-zero, we make a schematic view of the grout agent appearance in **Fig. 13**a). The measured data are shown in **Fig. 13**b). While the depth at which grout agents appear is different, the simulation reproduces the appearance, except cases from Stage 8 to the check A and check B. It should be mentioned that the difference in the

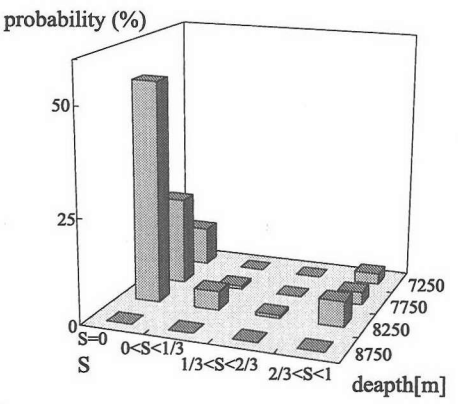

Fig. 12 Probability of Grout Agent Appearance

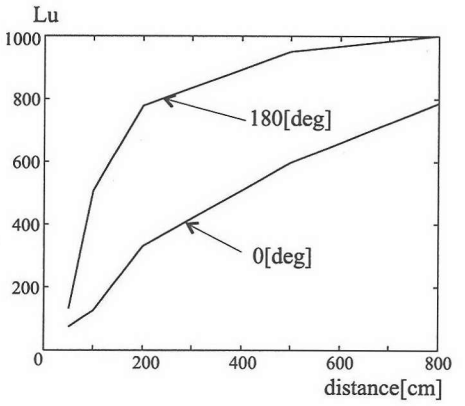

Fig. 14 Change of Lu

depth is probably due to a fact that well-developed cracks were not located on planes; regarding to the check B, for instance, the appearance at 40[m] from Stage 8 in **Fig. 13**a) corresponds to the appearance at 60[m] from Stage 8 in **Fig. 13**b).

As the validity of the MSFN is verified to some extent, we compute the spacial variation of Legion values, and show the variation in 0 and 180[deg] directions in **Fig. 14**. Major improvement in the permeability is observed up to 1[m] from the grouting hole. The better improvement for the 0[deg] direction is predicted; this is because cracks are developed in particular directions. The effects of the gravity on the permeable flow are completely neglected; it is relatively simple to modify the MSFN such that these effects are accounted.

(4) Change in Grout Specification

Finally, we simulate a fictitious grouting of different specifications, to see the change in the rock mass improvement. For simplicity, we consider a case when

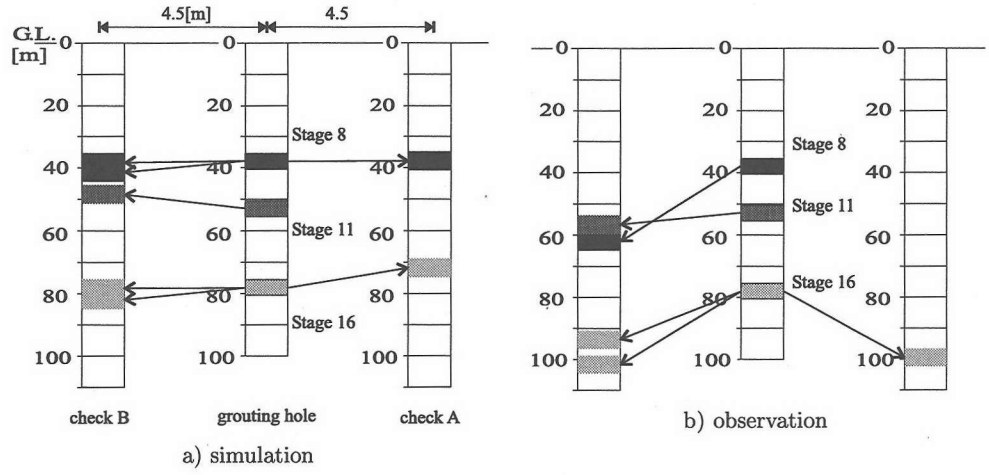

Fig. 13 Grouting Agents Appearing in Check Holes

Table 9 Studied Specification

spec.	1	2	3
t-P	×2.0	×10	×100

the input pressure[3] is increased; P is multiplied by 2, 10, and 100; see **Table 9**. The variation of Legion values in the 0 direction are plotted in **Fig. 15**. Here, we set $\alpha = 0.5$ as this value was obtained from the previous simulation. The rock mass improvement is predicted by increasing the applied pressure, although joints close to the grout hole are damaged due to high pressure.

One interesting application of the MSFN is that we can predict the grout pressure which is required to decrease Legion values to a desired value in a desired range. **Figure 16** shows this prediction; curves show the maximum distance within which Legion values are smaller than the specified[4] values. Such prediction of the grouting effects can support in determining grout specifications. It should be emphasized that **Fig. 16** is one example of the MSFN application, and the accuracy of this prediction is not verified.

4. CURTAIN GROUTING OF RTIA

The basic validity of the RTIA is first examined by carrying out simple numerical simulations of partially open parallel disks. Then, the data of the curtain grouting used in the previous section are used in the

[3] It is more realistic to use a t-Q relation as input data instead of a t-P relation.

[4] Legion values specified in this example are much larger than ordinarily desired values such as 2.

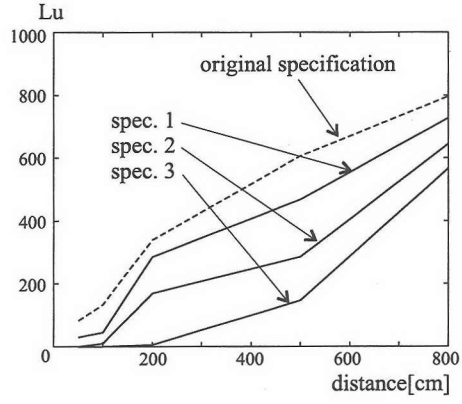

Fig. 15 Change of Lu for Different Spec.

RTIA to evaluate the water channel conditions and the distance of grout agents in actual sites. The RITA evaluates the width which is filled with the grout agent (W) and the distance at which the grout agent flows (R), using the t-P-Q relation. These W and R are given as a function of the distance from the center (r) and the time (t), W(r) and R(t); see Appendix. These evaluations are compared with the prediction of the MSFN.

(1) Simulation Using Generated Data

In order to see the basic validity, we apply the RTIA to partially open parallel disks which are numerically generated. As a model of well and poorly connected water channels, a linear function of $\sqrt{r}$ (good connectivity) and a trigonometric function of r (poor connectivity) are used to prescribe W. A t-P relation of the curtain grouting is applied to compute a t-Q relation

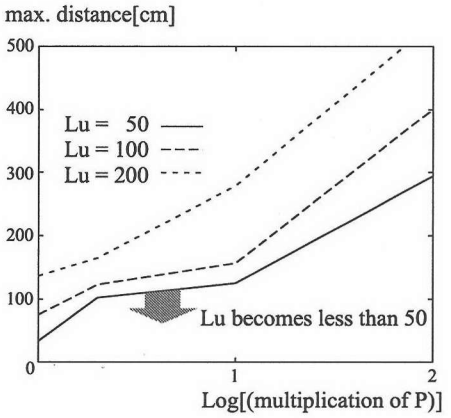

Fig. 16 Estimation of Range Improved by Grouting

Table 10 Thickness of Disk

stage	8	11	16
h[cm]	0.08	0.02	0.51

for these disks, and then we take the inversion of a t-W-R relation from this t-P-Q relation. No errors are added in the t-P-Q relations. **Figure 17** shows the assumed and inverted r-W relations.

As is seen, the inversion from t-P-Q to t-R-W is satisfactory. In particular, the increase and decrease in the R-W relation are well reproduced in **Fig. 17**b). This is due to the well-posedness of the inverse problem, as it is solved by a simple linear analysis of the measured data except for the loss of the accuracy in integrating the rate of R and W with respect to time.

(2) Simulation Using Measured Data

Using t-P-Q relations which were measured during the curtain grouting of Stages 8, 11, and 16, we carry out the RTIA to evaluate a t-R-W relation. The thickness of the parallel disk is given as the sum of the width of observed well-developed cracks; see Table 10. As a typical example, **Fig. 18** plots the r-W and t-R relations computed for Stage 16. Wild changes in the r-W relation are due to the fluctuation of the measured t-P-Q relation. It is seen that the water channel becomes a pipe-like as W becomes constant for larger r, and that the distance of the grout intrusion increases monotonically with respect to the time t.

In the partially open parallel disk model, W is an open range in which grout agents flow. We can consider that W can be connected to the saturation ratio, S, of the MSFN, as S tells the amount of grout agents running into joints. Taking the average of S in all directions, we obtain an r-S relation and compare it with

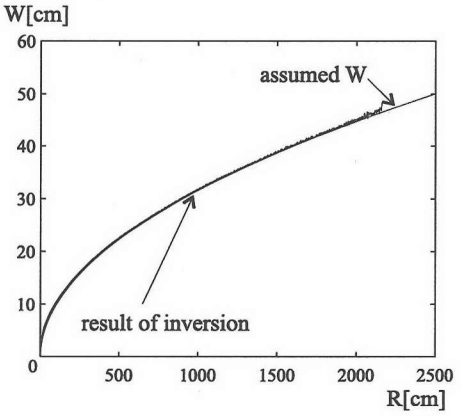

a) case of good connectivity

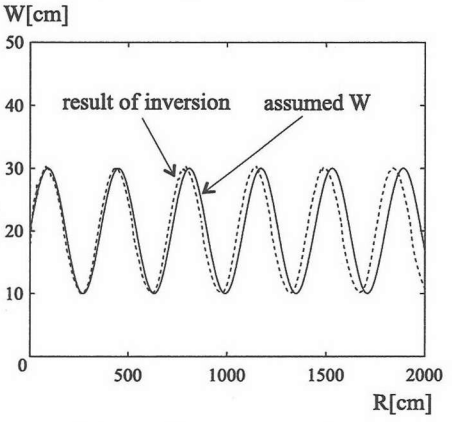

b) case of poor connectivity

Fig. 17 Numerical Simulation of Inversion

an r-W relation. The results for all the three stages are plotted in **Fig. 19**, where W and S are normalized by the values at r=10[cm]. As is seen, the profile of these relations are close to each other. In particular, the maximum distance of the grout agents predicted by the RTIA coincides with the maximum distance of non-zero S of the MSFN. This agreement may suggest the validity of the RTIA, and the RTIA is potentially applicable[5] to practical usage in evaluating the conditions of grouting which is being applied.

5. CONCLUDING REMARKS

While the validity of the MSFN and RTIA are not fully verified, we obtain several numerical results which support the basic validity to some quantitative extent. Further investigation is definitely required to examine the validity as well as the usefulness. We

[5] This will require accurate evaluation of h or some interpretation of the computed t-R-W relation.

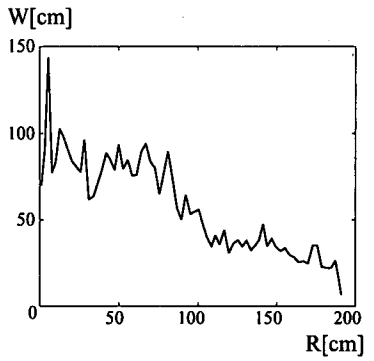

a) r-W

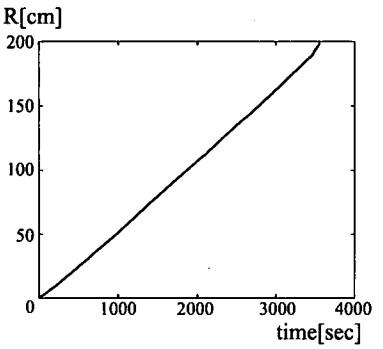

b) t-R relation

Fig. 18 Typical Results of Inversion

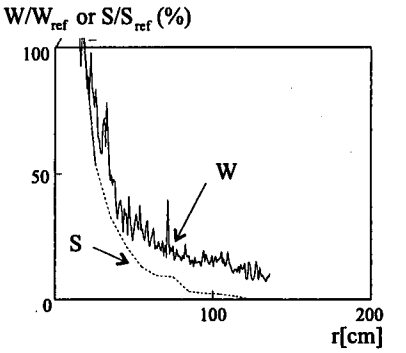

a) Stage 8

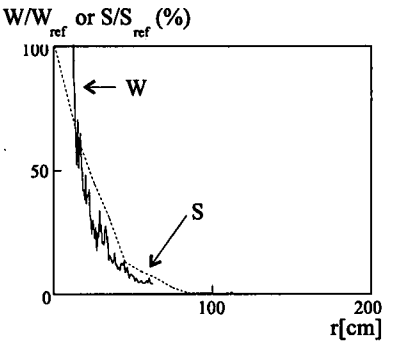

b) Stage 11

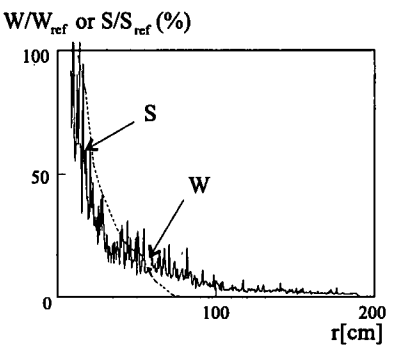

c) Stage 16

Fig. 19 Comparison of W of RTIA with S of MSFN

are considering the following two investigations: 1) establish rational interpretations of the prediction of the MSFN, evaluating the standard deviation of the results (it will be necessary to determine how many stand deviation should be added/subtracted from the average in order to account for the local variation of cracks and water channels); 2) apply the RTIA to monitor the real-time grout condition such as the distance to which grout agents reach or the connectivity of water channel (the RTIA can be a vital tool for grouting since it is possible to install the RTIA to a grouting apparatus as it requires a simple integration of continuously measured data).

APPENDIX: GROUT ANALYSES

The MSFN analyzes the permeable flow running through a fracture network which is randomly generated according to the geological data. The network consists of circular-disk-shaped joints with constant thickness, which are mutually connected through intersections. Assuming the Poiseulle flow, we can compute the permeable flow in the network just determining the pressure and flux at all intersections. This leads to a simple matrix equation for the intersection pressure, and the matrix components can be analytically determined like the finite element method. The MSFN considers the non-linear behavior of the t-P-Q relation, making two models, the elastic and inelastic deformation of joints due to the grout pressure and the stacking and hardening process of grout agents in joints. These models introduce unknown parameters, α and β, as

$$\mathrm{d}h/\mathrm{d}P = -\alpha k, \quad \mu = \mu^{\circ}(1 + \beta(t/h)),$$

where h and P are the joint thickness and pressure,

and k is the elastic stiffness computd from the joint shape, and μ and μ° are the current and initial viscosity, and t is the intruded time. The MSFN also evaluates the grouting effects as the reduction of the joint thickness due to the intruded grout agents, and the third unkown parameter γ is introduced as

$$\Delta h' = -\gamma S,$$

where $\Delta h'$ and S are the reduction of the joint thickness and the volume fraction of the agent in the joint.

The RTIA predicts the water channel conditions and the grout filling, modeling a water channel as a partially opened paralle disk. The thickness is set as constant, h, and the radius is sufficiently large. The water channel conditions are represented by the change of the part of the disk in which the grout agents flow, and the grout filling is evaluated as the distance at which the grout agent reaches. As mentioned, this problem setting leads to the inversion of the r-W relation (the distance and the width filled with grouting) and t-R relation (the time and the distance) from the measured t-P-Q relation, as follows:

$$\frac{\mathrm{d}R}{\mathrm{d}t}(t) = \sqrt{\left(\frac{1}{k} - \frac{1}{k'}\right)^{-1} Q(t) \frac{\mathrm{d}}{\mathrm{d}t}\left(\frac{P(t)}{Q(t)}\right)},$$

$$W(R) = \sqrt{\left(\frac{1}{k} - \frac{1}{k'}\right)^{-1} \frac{1}{h^2} \frac{Q(t)}{\frac{\mathrm{d}}{\mathrm{d}t}\left(\frac{P(t)}{Q(t)}\right)}},$$

where k and k' are the permeability of water and the grout agent. Thus, the width (W) at the distance (R) are determined.

REFERENCES

1) Baker, J.: *J. Water Resor. Res.*, Vol. 24, No. 10, pp. 1796-1804, 1988.
2) Cacas, M.C.: Modeling fracture flow with a stochastic discrete fracture network: calibration and validation 1. flow model, *Water Resor. Res.*, Vol. 26, pp. 479-489, 1990.
3) Hori, M. and Koyama, T.: Numerical analysis method of grouting based on fracture network analysis, *Proc. 42nd Sympo. on Geomechanics*, pp. 37-42, 1998 (in Japanese).
4) Hori, M. and Koyama, T.: Proposal of two grout analysis methods, *JSCE*, 1999 (in print).
5) Long, J.C.S., Remer, J.S., Wilson, C.R. and Witherspoon, P.A.: Porous media equivalents for networks of discontinuous fractures, *J. Water Resour. Res.*, Vol. 18, No. 3, pp. 645-658, 1982.
6) Morita, Y., Sugimura, Y. and Watanabe, K.: Channel network model for dam foundation rock, *Proc. 27th Sympo. on Rock Mechanics*, pp. 234-238, 1997.
7) Nagayama, I. and Yoshinaga. K.: Consideration of grouting characteristics of dam foundation (cracked dam), *Proc. 16th Sympo. on Rock Mech.*, pp. 310-314, 1984 (in Japanese).
8) Oda, M. Hatsuyama, Y. and Ohnishi, Y.: Numerical experiments on permeability tensor and its application to jointed granite at Stripa Mine, Sweden, . *J. Geological Res.*, Vol. 92, No. B.8, pp. 8037-8048, 1987.
9) Sibson, R.H.: Structural permeability of fluid-driven fault-fracture meshes, *J. Struct. Geol.*, Vol. 18, No. 8, pp. 1031-1042, 1996.
10) Yamaguchi, K., and Matsumoto, T.: Permeability of dam foundation and Legion values, *JSCE*, III, No. 412, pp. 51-62, 1992.

(Received June 15, 1998)

二つのグラウト解析によるグラウチングのシミュレーション

堀宗朗・小山高寛

本論文はグラウチングに対する二つの解析手法，モンテカルロシミュレーションを利用したフラクチャーネットワーク解析 (MSFN) とリアルタイムインバージョン解析 (RTIA) の妥当性を検証する．MSFN は所定の仕様のグラウチングによる改良効果を予測するもので，コンソリデーションとカーテングラウチングのシミュレーションの結果，1) 注入圧-注入量関係，2) ルジオン値の低下，3) グラウト剤の流出，に関して実測データとある程度の一致をみた．RITA は計測された注入圧-注入量関係をもとにグラウト孔近くの水みちとグラウト剤到達距離を逆解析するもので，コンソリデーショングラウチングに対するシミュレーションを行った．